

Deep-learning based Tools for Automated Protocol Definition of Advanced Diagnostic Imaging Exams

Andrew S. Nencka, Mohammad Sherafati, Timothy Goebel, Parag Tolat and Kevin M. Koch

SafeNet Consulting, Milwaukee, WI

Department of Radiology, Medical College of Wisconsin, Milwaukee, WI

ARTICLE INFO

Keywords:

Protocols, machine learning, quality improvement, automation, natural language processing, deep learning

ABSTRACT

Purpose: This study evaluates the effectiveness and impact of automated order-based protocol assignment for magnetic resonance imaging (MRI) exams using natural language processing (NLP) and deep learning (DL).

Methods: NLP tools were applied to retrospectively process orders from over 116,000 MRI exams with 200 unique sub-specialized protocols (“Local” protocol class). Separate DL models were trained on 70% of the processed data for “Local” protocols as well as 93 American College of Radiology (“ACR”) protocols and 48 “General” protocols. The DL Models were assessed in an “auto-prototyping (AP)” inference mode which returns the top recommendation and in a “clinical decision support (CDS)” inference mode which returns up to 10 protocols for radiologist review. The accuracy of each protocol recommendation was computed and analyzed based on the difference between the normalized output score of the corresponding neural net for the top two recommendations.

Results: The top predicted protocol in AP mode was correct for 82.8%, 73.8%, and 69.3% of the test cases for “General”, “ACR”, and “Local” protocol classes, respectively. Higher levels of accuracy over 96% were obtained for all protocol classes in CDS mode. However, at current validation performance levels, the proposed models offer modest, positive, financial impact on large-scale imaging networks.

Conclusions: DL-based protocol automation is feasible and can be tuned to route substantial fractions of exams for auto-prototyping, with higher accuracy with more general protocols. Economic analyses of the tested algorithms indicate that improved algorithm performance is required to yield a practical exam auto-prototyping tool for sub-specialized imaging exams.

arXiv:2106.08963v1 [cs.LG] 28 May 2021

 anencka@mcw.edu (A.S. Nencka)

ORCID(s): Andrew S. Nencka (0000-0001-5268-2718); Mohammad Sherafati (0000-0001-5362-7550); Timothy Goebel (); Parag Tolat (0000-0003-1260-5456); Kevin M. Koch (0000-0003-4490-9761)

1. INTRODUCTION

Health care expenditures in the United States (US) represent more than 19% of its gross domestic product. This is approximately twice that of other high-income countries, with a similar outcome in life expectancy [1, 2, 3]. Advanced imaging, including computed tomography (CT) and magnetic resonance imaging (MRI), strongly contributes to health care costs. Notably, the number of MRI exams per 1,000 residents in the US has doubled over the past two decades [4].

The imbalance between imaging costs and diagnostic benefits is rooted in the inappropriate utilization of imaging resources. Inefficiencies have motivated reforms in imaging utilization which support evidence-based imaging [5] and utilize clinical decision support (CDS) systems [6, 7]. Computerized physician order entry [8, 9] software tools have provided evidence supporting improved process outcomes. These outcomes include both guideline adherence [10] and reduced imaging overuse [11].

Though CDS algorithms offer appropriate “general” imaging protocols (e.g. contrast-enhanced imaging in malignant disease), they do not currently model more complex, advanced sub-specialized imaging protocols that require expert radiologist intervention.

In a value-oriented radiology model, protocol selection, a non-interpretive task, takes place before image acquisition, diagnostic interpretation, and report completion [12]. Protocol selection takes up to 6% of a radiologist’s time and is a frequent source of interruptions [13]. It is also labor-intensive, requiring the choice of imaging modality and planes, contrast agent, acquisition parameters, acquired series, and anatomical area covered.

Such complexity causes protocol variation [14] due to individual radiologist practices and preferences. This variation leads to decreased imaging appropriateness, increased interpretive time, and less optimal outcomes. This has motivated the development of tools to standardize protocol construction [15]. Standardization aligns with the principles of Imaging 3.0™: appropriateness, quality, safety, efficiency, and patient experience [16].

Radiologic technologists rarely change protocols from an ordered advanced imaging exam. Furthermore, the overall change rate for radiologists and residents for the most commonly ordered CT and MRI studies is similarly very low. These factors have led experts to conclude that order entry protocol selection is amenable for automation [17].

Machine learning and deep learning (DL) [18] can be leveraged with information from orders and patients’ electronic medical records (EMRs) to train artificial intelligence (AI) models to predict protocols from new orders. Robustly auto-protocolling sub-specialized exams could a) reduce the expert effort in protocolling exams, b) enable workflows for patient self-scheduling advanced exams, c) simplify the use of sub-specialized protocols, d) reduce error arising from interrupting radiologist interpretive workflows, and e) expand time for radiologists to perform more valuable tasks.

The growth of AI applications in interpretive and non-interpretive radiology has been extensively reviewed [19, 20].

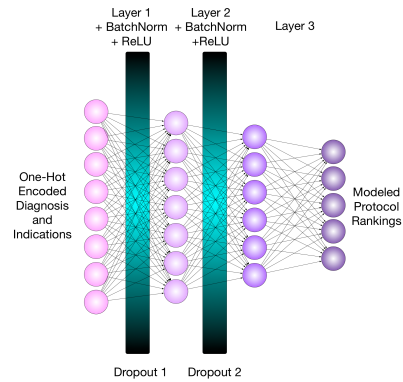


Figure 1: The fully connected neural network utilized in this study for MRI order protocolling. A one-hot encoded input vector of indication and diagnosis words is input, and vector scoring each protocol is output. Dropout and batch normalization layers are included to improve performance with limited training data.

Related to this work, AI-DL-based models have been employed for protocol assignment and quality improvement, demonstrating promising results in neuroradiology [21, 22] and musculoskeletal MRI [23, 24]. Recently, Karla *et al.* [25] demonstrated an AI-augmented workflow to automate CT and MRI protocolling for 69% of orders in a moderately sized sample from a homogeneous clinical environment. They showed >95% concordance with radiologists in those cases, and provide 92% accuracy in top-three protocol suggestion for the remaining cases.

Here, a similar exam protocolling technique is presented and analyzed. This algorithm uses physician-provided indications for imaging and associated *a priori* diagnoses noted in the EMR. The present work holds some key distinctions from the study presented by Karla *et al* [25]. First, the application in this work is both more specialized and targeted at a diverse patient population. While previous work considered both CT and MRI, the present work exclusively considers MRI examinations from a data bank that is over six times larger than the combined MRI and CT dataset used by Karla *et al.* [25]. Additionally, the considered patient population is extracted from an academic hospital network serving a more diverse urban and suburban population compared to the previously studied sample from a Veterans Administration hospital. Finally, this work provides an economic analysis of the technology to illustrate the impact of implementing such technology in a large imaging network.

2. METHODS

2.1. Data Source and Preparation

De-identified MRI protocols and matched free-text indications and diagnoses for the 2018 and 2019 calendar years were extracted from the EMRs of an academic hospital network through an IRB-approved data bank. This yielded 116,224 unique imaging exams.

Minimal pre-processing was performed prior to network

training to emulate a real-world application. In pre-processing all characters were set to lower case, stop removed using the Natural Language Toolkit (NLTK) “english” corpus module [26]), and punctuation removed.

Due to the preferential use of MRI for neurologic and orthopedic diagnostics, data were class imbalanced across all potential protocols. The `train_test_split` function in *Scikit-learn* [27] yielded a class-balanced 70%/30% training/test split of the dataset.

For each order, indications and diagnoses were encoded with a “one-hot encoding” scheme [27] of all words identified in those fields of the training set. The encoded vector included the concatenation of separate vectors for the indication field (19,212 elements) and diagnosis field (4,615 elements). Words in the testing set which were not included in the training set were removed.

Table 1: Prevalence of the five most common protocols for each class of protocols in the considered clinical data set.

General	ACR	Local
Spine without contrast 24.7 %	Lumbar spine without contrast 17.6 %	Lumbar spine without contrast 13.9 %
Head with and without contrast 17.9 %	Head without and with contrast 11.6 %	Brain with and without contrast 11.6 %
Knee without contrast 8.4 %	Cervical spine without contrast 8.6 %	Cervical spine without contrast 8.6 %
Head without contrast 8.1 %	Knee without contrast 8.4 %	Brain without contrast 5.8 %
Spine with and without contrast 7.8 %	Head without contrast 6.8 %	Abdomen without and with contrast 4.9 %

2.2. Model Design and Training

All 200 “Local” protocols were mapped to 93 protocols defined by the American College of Radiology (“ACR”) “Appropriateness Criteria”[®] [28]. Subsequently, each ACR protocol was mapped to one of 48 more “General” protocols. A full mapping of protocols is provided in the supplemental material.

Three fully connected neural networks were designed to ingest the indication and diagnosis vector and return a vector of n scores, where n is the number of protocols in the protocol class. The recommended protocol is the element with the greatest returned value. Figure 1 illustrates this neural network. It included 23,827 inputs (corresponding to each encoded word), and three dense layers with $4n$, $2n$, and n neurons [29]. The network also utilized rectified linear unit (ReLU) [30] activations, 50% training dropout [31] layers,

and batch normalization [32].

One network was trained for each set of protocols using an NVIDIA (Santa Clara, California) Titan V graphical processing unit (GPU), an ADAM optimizer with a learning rate of 0.0001 [33], a cross-entropy loss function [34], and two hundred training epochs with data shuffling. Using five data loading threads and a batch size of 24 orders, each training epoch lasted approximately 32 seconds. Inference on test data with a batch size of 24 orders took 0.7 ms per order.

2.3. Modes of Operation and Performance Metrics

Two modes of inference use were defined: auto-protocolling (AP) and clinical decision support (CDS). As an AP tool, the top recommendation was returned as the selected protocol. In the CDS mode, the top five recommendations were returned as a set of proposed protocols to be evaluated by a protocolling radiologist/technologist.

Relative amplitude differences of inferred protocol weightings were used to switch between AP and CDS modes. Each output vector was scaled to have a minimum of zero and a total sum of 1.0. The difference between the top recommendation and the second recommendation was computed, and is defined as “delta” which is shown in Fig. 2. The delta can be interpreted as a rough indicator of confidence in the recommended protocol, with a larger value of the delta corresponding to greater confidence for the selected protocol. All reported metrics were computed as a function of delta values.

A rudimentary analysis of the economic impact of using these models was performed based upon the percentage of exams that are routed through the AP model. This analysis assumed an average hourly rate of \$38 (technologist) and \$206 (radiologist) (salary.com), an average time to protocol an exam of two minutes (technologist) and one minute (radiologist), and an annual volume of 58,000 exams. Cost savings were computed as the fraction of auto-protocolled exams multiplied by the annual exam volume, time to protocol an exam, and practitioner’s hourly rate.

3. RESULTS

Each model was used to inference the test data set of 34,868 orders. Each protocol was assigned a percentile score for the order. The known protocol acquired in the test data set was then compared to the percentile rank for that protocol in the inferred protocol vector. Histograms of percentile rankings of correct protocols for each of the three AP models are illustrated in Fig. 3.

The delta threshold can be tuned depending upon a site’s preference for acceptable levels of discordance between AP and manual results along with the volume of orders routed through the AP workflow. For a given magnitude of the delta, in Fig. 4, all the “AP–” exams below the threshold were protocoled incorrectly and would be appropriately routed to CDS mode for radiologist protocolling. Similarly, “AP+” orders above this threshold were auto-protocolled correctly and would utilize the AP workflow, as desired.

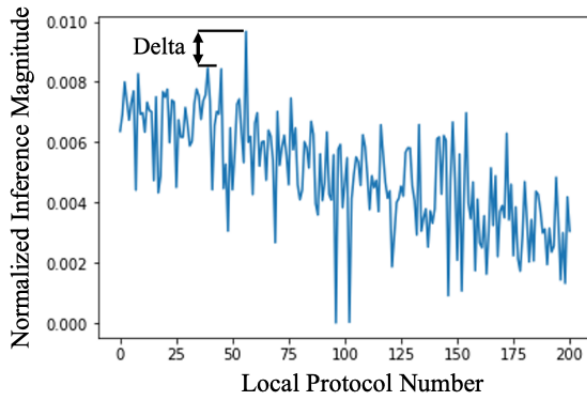


Figure 2: Normalized output of the “Local” model. The magnitude of the rough confidence metric, “delta,” is shown as the difference between the top two inferred magnitudes.

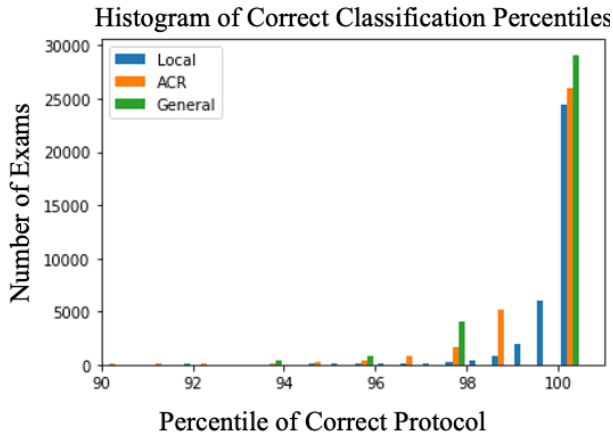


Figure 3: Histograms of percentile rankings of correct protocols for each AP model.

Table 2: Accuracy of the modeled recommended protocols based on a test dataset of 34,868 orders. If used in pure auto-protocolling mode, the top recommendation indicates the percentage of exams wherein the auto-protocolling results were correct. If used in pure clinical decision support (CDS) mode, the top five recommendation indicates the percentage of exams wherein the desired protocol is in the list of returned protocols. If CDS were expanded to return 10 protocols, the final row illustrates the resulting accuracy.

Accuracy Metric	Protocol Class		
	General	ACR	Local
Top Recommendation	82.8%	73.8%	69.3%
Top Five Recommendation	98.6%	97.0%	96.0%
Top 10 Recommendation	99.4%	98.7%	98.0%

A well-performing AP model yields a bimodal histogram with larger areas of AP+ and AP− distributions lying above and below the threshold, respectively. For example, histograms shown in Fig. 4 with a shift of the “AP+” distribution towards higher deltas with more general protocols suggest that generalized protocols are better suited for the AP workflow.

Figure 5 illustrates the increasing accuracy of AP models as a function of the delta. With small delta values, the performance of the AP mode is improved with more general sets of protocols. This trend is reversed with higher delta values. If a high rate of accuracy is desired for AP workflows, more protocols that are more specific and are thresholded with higher delta values are preferable, although this results in a low percentage of exams that proceed through the AP workflow.

The percent of cases with the correct protocol in the top five recommendations of the models’ CDS mode is illustrated in Fig. 6. With a smaller set of general protocols, there is a higher probability of the correct protocol being in the top recommendations, and the “General” model outperforms the other models across all considered delta thresholds. As delta increases, the performance of the CDS mode improves. The highly specialized “Local” model outperforms the more general “ACR” protocolling model with a delta threshold between 0.0006 and 0.0020.

3.1. Economic Impact Analysis

The fraction of exams that are routed to AP mode for each protocol class monotonically decreases with the increase of delta as shown in Fig. 7. This decay is faster for the sub-specialized protocols. For general protocols, a higher volume of exams can be routed through the auto-protocolling workflow irrespective of the delta. For sufficiently small delta (~ 0.0002), over 80% of exams can be routed to AP mode, irrespective of the model utilized.

Economic impact analysis of these results suggests that modest cost savings can be achieved using these DL-based protocolling algorithms. Approximately 25% of a technologist or 12.5% of a radiologist full time equivalent employee (FTE) can be saved with a delta threshold of 0.10 using the sub-specialized “Local” model which achieves over 95% accuracy in its CDS mode and nearly 95% accuracy in its auto-protocolling mode. While these savings are not inconsequential, they are not substantially impactful on the budget of the large healthcare imaging network utilized for the present study.

More substantial savings could be achieved if less specialized protocols are used, enabling the auto-protocolling workflow to be employed more often, with the “General” model achieving over 90% accuracy in AP mode, 97% accuracy in CDS mode, and over 150% or 37% technologist or radiologist FTE savings with a delta threshold of 0.0016.

Overall, these results highlight the need for future work to render the evaluated technologies viable in clinical enterprises relying on specialized exam protocols.

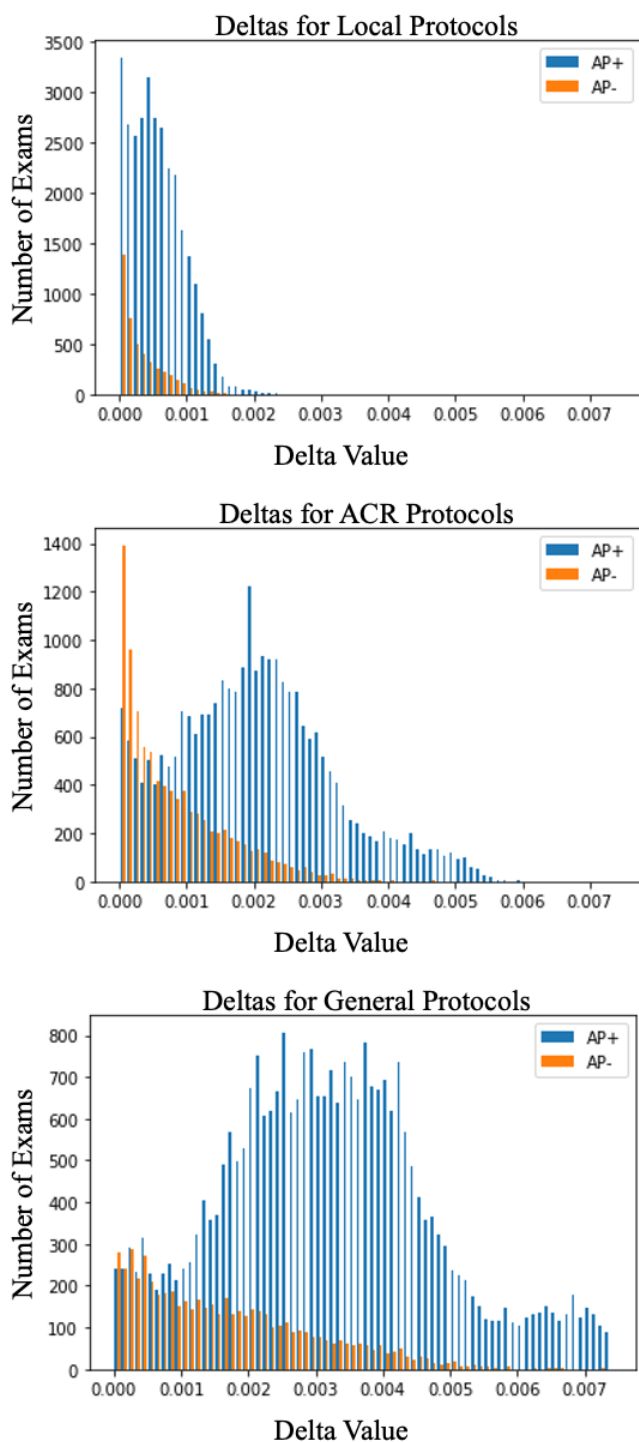


Figure 4: Histograms of delta for each AP model when the AP recommendation was correct (AP+) and incorrect (AP-)

4. DISCUSSION

In this feasibility study, AI-based algorithms were developed and tested to automate order-based protocoling for 116,224 MRI exams ordered during 2018 and 2019 in an urban and suburban imaging network.

Table 2 illustrates that the evaluated models are not suf-

ficient as pure AP tools. This is likely due to the diverse patient population and limited information contained in physician order notes. If used for protocol recommendation in a CDS capacity, wherein five to 10 protocols are recommended to an individual protocoling the exam, the models perform very well. Furthermore, if generalized exam protocols are utilized, model performance improves. The results shown in Figs. 3 through 7 suggest the use of an alternative hybrid solution, wherein AP is performed if a key metric is above threshold and CDS is offered below this threshold.

Rudimentary economic impact analysis of the singular AP/CDS modes evaluated in this study predicts modest cost savings when implementing such approaches. This economic impact performance is highly dependent on the algorithmic performance in the AP mode on the specialized exam protocol pool.

The accuracy of the AP workflow for specialized protocols shown in this work is lower than in other work and the observed delta threshold is not as sharp as that reported in Kalra et al[25], which focused on a population of primarily older males in a single hospital in the Veterans Administration system. In contrast, the present study utilized data from a large urban-based academic medical system serving a broad range of patients. Of note, the broader and more diverse dataset utilized in this study, along with the categorical analysis of exam protocols with increasing specificity, enabled the practical economic analysis that is unique to the present study.

The primary errors in the AP mode of the evaluated models in this study occurred when predicting highly specific protocols. In protocols that were lateralized (i.e. right versus left wrist), protocol errors primarily indicated the appropriate anatomy and contrast agent usage while incorrectly indicating laterality. This could be addressed by adding an ordering question to the electronic medical record software to indicate exam laterality. In protocols which were not lateralized, and included options regarding contrast agent inclusion (i.e. without, with and without, or with contrast), most errors again included correct anatomy and incorrect contrast agent selection. There are cases wherein the inclusion of contrast agent would be optimal for imaging but detrimental for the patient (i.e. pregnant patients and patients with acute renal injury [35]), which may contribute to this error. The addition of model inputs based upon the medical record to gain information regarding contraindications for contrast agent usage could further improve model performance.

The financial analysis included in this study highlights the need for additional informatics integration, such as the aforementioned order laterality and contrast agent specifications, that must be utilized in combination with the demonstrated DL-based algorithms to improve performance. Without improved inputs to AP algorithms, it is unlikely that such tools will offer a substantial benefit to radiology practices. However, it is noted that the addition of such information to the neural network inputs is not a substantial roadblock and is likely to provide a viable path forward in the development of AP workflows.

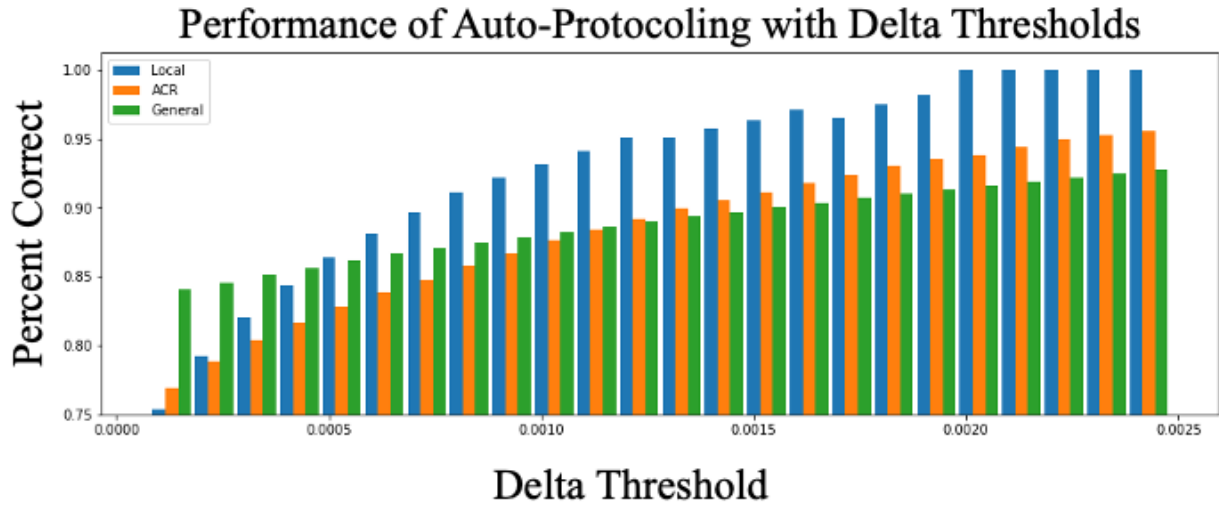


Figure 5: Bar chart of percentage of correct AP recommendations as a function of delta for each model

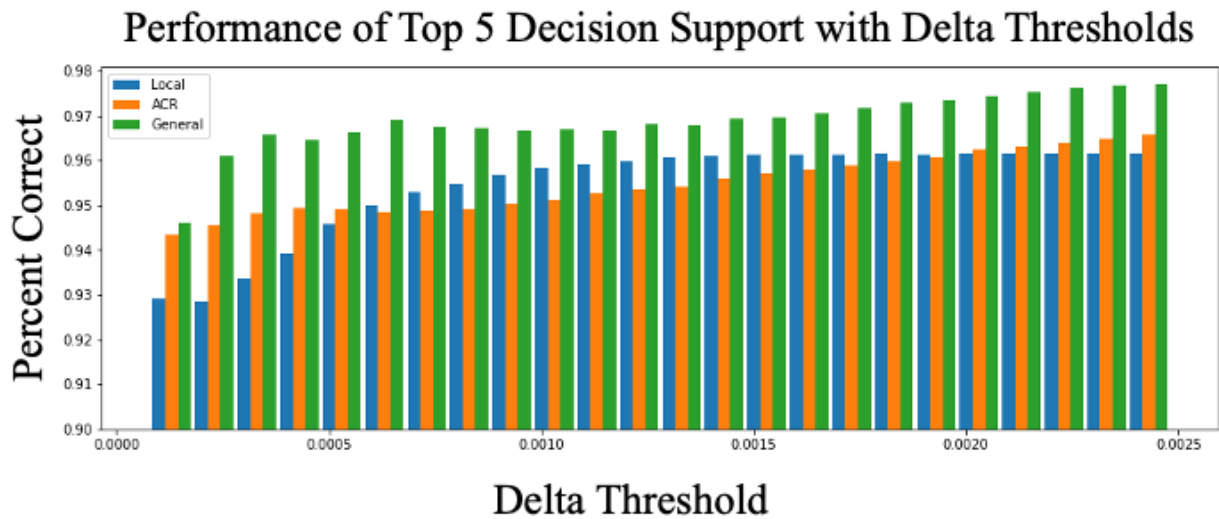


Figure 6: Bar chart of percentage of CDS recommendations containing the correct protocol as a function of delta for each model

The present study shows that DL-based AP technology can be designed to relieve a portion of the manual protocoling burden which can interrupt interpretive work. Such interruptions cause frustrations and lead to increased exam reporting times or potential errors in image interpretations [36,

37, 38, 13, 39]. In addition, such a tool may provide radiologists with increased uninterrupted time. Recent work supports this hypothesis[40], whereby a simple AP intervention providing a standardized CT protocoling system for emergency exams can improve the radiology workflow by reduc-

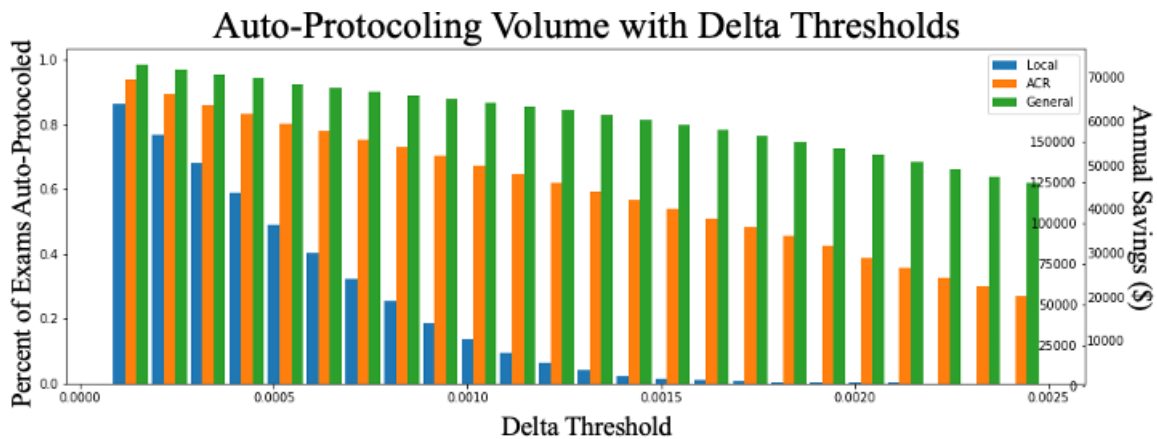


Figure 7: Bar chart of the AP model case volume. The vertical axis on the left indicates the fraction of exams in the test data set which are routed through the AP model for the “delta” threshold indicated along the horizontal axis. The right vertical axis indicates the estimated annual cost reduction associated with the auto-protocoling tool usage if radiologists primarily perform protocoling duties (scale to left of axis) or technologists (scale to right of axis).

ing the lag time between ordering and protocoling, and improving time to the final report. Moreover, that work demonstrated improvements in radiology residents’ work satisfaction and wellness when such tools are utilized.

The present study has two main limitations: 1) source data was limited to a single hospital network and 2) neural network evaluation was performed on retrospective data. While the trained models are not necessarily appropriate for application to data in a different hospital network, the model architecture, bifurcated workflow, and delta analysis are directly transferable. As a result, real-time assessment of discrepancies between radiologist prescriptions and algorithm recommendations is not captured, and temporal savings associated with a CDS list of proposed protocols is not measured. Neural network hyperparameters were determined through a cursory grid search, and more formal consideration of network architecture could hold value. Further accuracy improvements are feasible through the increases in data extracted from the EMR for model inputs. The economic analysis performed in this study only accounts for the time spent protocoling of exams. It does not take into account further benefits of the evaluated technology, such as improved interpretive productivity and reduced protocoling time with CDS usage.

5. CONCLUSIONS

Exam protocol selection for advanced diagnostic imaging exams is a monotonous and unbilled use of professional resources. The present study demonstrates that DL-based AP and CDS tools offer the potential to alleviate these resource demands. By tuning a threshold for switching between AP and CDS modes, compromises between cost savings and protocol accuracy can be modulated. Despite the encouraging preliminary demonstration of DL-based AP of advanced imaging exams, economic analyses suggest that substantially improved algorithm performance will be re-

quired to yield a practical AP tool for sub-specialized imaging exams. Specific additional inputs to the models, including laterality and patient-specific contrast contraindications, are hypothesized to enable such performance improvements.

TAKE-HOME POINTS

- Deep learning-based automated diagnostic imaging exam protocoling is feasible in a diverse clinical network.
- The performance of such algorithms depends on the level of specificity of pre-defined exam protocols.
- The output of AP algorithms can be thresholded to modulate exam volume between AP and CDS tools.
- Economic analysis of purely order-driven models suggests that increased levels of information will be required as inputs to trained models before such algorithms are viable for clinical usage.

6. ACKNOWLEDGMENTS

The authors thank Robin Ausman and Bradly Swearingen for their work to extract the data utilized in this analysis, as well as Jess Zieman and Jeff Rehm for support regarding the financial aspects of this work.

7. BACKMATTER

References

1. Truffer, C.J., Keehan, S., Smith, S., Cylus, J., Sisko, A., Poisal, J.A., Lizonitz, J., Clemens, M.K.. Health spending projections through 2019: The recession’s impact continues. *Health Affairs* 2010;29(3):522–529. URL: <https://doi.org/10.1377/hlthaff.2009.1074>. doi:10.1377/hlthaff.2009.1074. arXiv:<https://doi.org/10.1377/hlthaff.2009.1074>; PMID: 20133357.
2. Chen, A., Goldman, D.. Health care spending: Historical trends and new directions. *Annual Review of Economics* 2016;8(1):291–319. URL: <https://doi.org/10.1146/annurev-economics-080315-015317>.

- doi:10.1146/annurev-economics-080315-015317.
arXiv:https://doi.org/10.1146/annurev-economics-080315-015317.
3. Papanicolas, I., Woskie, L.R., Jha, A.K. Health Care Spending in the United States and Other High-Income Countries. *JAMA* 2018;319(10):1024–1039. URL: https://jamanetwork.com/journals/jama/fullarticle/2674671. doi:10.1001/jama.2018.1150; publisher: American Medical Association.
 4. Health care use - Magnetic resonance imaging (MRI) exams - OECD Data. URL: http://data.oecd.org/healthcare/magnetic-resonance-imaging-mri-exams.htm; library Catalog: data.oecd.org.
 5. Medina, L.S., Blackmore, C.C.. Principles of Evidence-Based Imaging. In: Medina, L.S., Blackmore, C.C., eds. *Evidence-Based Imaging: Optimizing Imaging in Patient Care*. New York, NY: Springer. ISBN 978-0-387-31216-3; 2006:1–18. URL: https://doi.org/10.1007/0-387-31216-1_1. doi:10.1007/0-387-31216-1_1.
 6. Khorasani, R.. Clinical Decision Support in Radiology: What Is It, Why Do We Need It, and What Key Features Make It Effective? *Journal of the American College of Radiology* 2006;3(2):142–143. URL: https://www.jacr.org/article/S1546-1440(05)00349-2/abstract. doi:10.1016/j.jacr.2005.11.008; publisher: Elsevier.
 7. Thrall, J.H.. Appropriateness and Imaging Utilization: “Computerized Provider Order Entry and Decision Support”. *Academic Radiology* 2014;21(9):1083–1087. URL: http://www.sciencedirect.com/science/article/pii/S1076633214001846. doi:10.1016/j.acra.2014.02.019.
 8. Ip, I.K., Schneider, L.I., Hanson, R., Marchello, D., Hultman, P., Viera, M., Chiango, B., Andriole, K.P., Menard, A., Schade, S., Seltzer, S.E., Khorasani, R.. Adoption and meaningful use of computerized physician order entry with an integrated clinical decision support system for radiology: Ten-year analysis in an urban teaching hospital. *Journal of the American College of Radiology* 2012;9(2):129 – 136. URL: http://www.sciencedirect.com/science/article/pii/S1546144011005928. doi:https://doi.org/10.1016/j.jacr.2011.10.010.
 9. Sutton, R.T., Pincock, D., Baumgart, D.C., Sadowski, D.C., Fedorak, R.N., Kroeker, K.I.. An overview of clinical decision support systems: benefits, risks, and strategies for success. *npj Digital Medicine* 2020;3(1):1–10. URL: https://www.nature.com/articles/s41746-020-0221-y. doi:10.1038/s41746-020-0221-y; number: 1 Publisher: Nature Publishing Group.
 10. Patterson, B.W., Pulia, M.S., Ravi, S., Hoonakker, P.L., Hundt, A.S., Wiegmann, D., Wirkus, E.J., Johnson, S., Carayon, P.. Scope and influence of electronic health record-integrated clinical decision support in the emergency department: A systematic review. *Annals of Emergency Medicine* 2019;74(2):285 – 296. URL: http://www.sciencedirect.com/science/article/pii/S0196064418314227. doi:https://doi.org/10.1016/j.annemergmed.2018.10.034.
 11. Blackmore, C.C., Mecklenburg, R.S., Kaplan, G.S.. Effectiveness of Clinical Decision Support in Controlling Inappropriate Imaging. *Journal of the American College of Radiology* 2011;8(1):19–25. URL: http://www.sciencedirect.com/science/article/pii/S1546144010003893. doi:10.1016/j.jacr.2010.07.009.
 12. Enzmann, D.R., Schomer, D.F.. Analysis of Radiology Business Models. *Journal of the American College of Radiology* 2013;10(3):175–180. URL: http://www.sciencedirect.com/science/article/pii/S1546144012005303. doi:10.1016/j.jacr.2012.09.001.
 13. Schemmel, A., Lee, M., Hanley, T., Pooler, B.D., Kennedy, T., Field, A., Wiegmann, D., Yu, J.P.J.. Radiology Workflow Disruptors: A Detailed Analysis. *Journal of the American College of Radiology* 2016;13(10):1210–1214. URL: https://www.jacr.org/article/S1546-1440(16)30191-0/abstract. doi:10.1016/j.jacr.2016.04.009; publisher: Elsevier.
 14. Boland, G.W., Duszak, R., McGinty, G., Allen, B.. Delivery of Appropriateness, Quality, Safety, Efficiency and Patient Satisfaction. *Journal of the American College of Radiology* 2014;11(1):7–11. URL: https://www.jacr.org/article/S1546-1440(13)00439-0/abstract. doi:10.1016/j.jacr.2013.07.016; publisher: Elsevier.
 15. Boland, G.W., Duszak, R.. Protocol Management and Design: Current and Future Best Practices. *Journal of the American College of Radiology* 2015;12(8):833–835. URL: https://www.jacr.org/article/S1546-1440(15)00325-7/abstract. doi:10.1016/j.jacr.2015.04.021; publisher: Elsevier.
 16. Imaging 3.0 | American College of Radiology. URL: https://www.acr.org/Practice-Management-Quality-Informatics/Imaging-3; library Catalog: www.acr.org.
 17. Tudor, J., Klochko, C., Patel, M., Siegal, D.. Order Entry Protocols Are an Amenable Target for Workflow Automation. *Journal of the American College of Radiology* 2018;15(6):854–858. URL: http://www.sciencedirect.com/science/article/pii/S1546144018301923. doi:10.1016/j.jacr.2018.02.003.
 18. LeCun, Y., Bengio, Y., Hinton, G.. Deep learning. *Nature* 2015;521(7553):436–444. URL: https://www.nature.com/articles/nature14539. doi:10.1038/nature14539; number: 7553 Publisher: Nature Publishing Group.
 19. Lakhani, P., Prater, A.B., Hutson, R.K., Andriole, K.P., Dreyer, K.J., Morey, J., Prevedello, L.M., Clark, T.J., Geis, J.R., Itri, J.N., Hawkins, C.M.. Machine Learning in Radiology: Applications Beyond Image Interpretation. *Journal of the American College of Radiology* 2018;15(2):350–359. URL: https://www.jacr.org/article/S1546-1440(17)31287-5/abstract. doi:10.1016/j.jacr.2017.09.044; publisher: Elsevier.
 20. Richardson, M.L., Garwood, E.R., Lee, Y., Li, M.D., Lo, H.S., Nagaraju, A., Nguyen, X.V., Probyn, L., Rajiah, P., Sin, J., Wasnik, A.P., Xu, K.. Noninterpretive Uses of Artificial Intelligence in Radiology. *Academic Radiology* 2020; URL: http://www.sciencedirect.com/science/article/pii/S1076633220300398. doi:10.1016/j.acra.2020.01.012.
 21. Brown, A.D., Marotta, T.R.. A Natural Language Processing-based Model to Automate MRI Brain Protocol Selection and Prioritization. *Academic radiology* 2017;24(2):160–166. URL: http://www.ncbi.nlm.nih.gov/pubmed/27889399. doi:10.1016/j.acra.2016.09.013.
 22. Brown, A.D., Marotta, T.R.. Using machine learning for sequence-level automated MRI protocol selection in neuroradiology. *Journal of the American Medical Informatics Association* 2018;25(5):568–571. URL: https://academic.oup.com/jamia/article/25/5/568/4569611. doi:10.1093/jamia/ocx125; publisher: Oxford Academic.
 23. Lee, Y.H.. Efficiency Improvement in a Busy Radiology Practice: Determination of Musculoskeletal Magnetic Resonance Imaging Protocol Using Deep-Learning Convolutional Neural Networks. *Journal of Digital Imaging* 2018;31(5):604–610. URL: https://doi.org/10.1007/s10278-018-0066-y. doi:10.1007/s10278-018-0066-y.
 24. Trivedi, H., Mesterhazy, J., Laguna, B., Vu, T., Sohn, J.H.. Automatic Determination of the Need for Intravenous Contrast in Musculoskeletal MRI Examinations Using IBM Watson’s Natural Language Processing Algorithm. *Journal of Digital Imaging* 2018;31(2):245–251. URL: https://doi.org/10.1007/s10278-017-0021-3. doi:10.1007/s10278-017-0021-3.
 25. Kalra, A., Chakraborty, A., Fine, B., Reicher, J.. Machine Learning for Automation of Radiology Protocols for Quality and Efficiency Improvement. *Journal of the American College of Radiology* 2020; URL: http://www.sciencedirect.com/science/article/pii/S154614402030288X. doi:10.1016/j.jacr.2020.03.012.
 26. Bird, S., Klein, E., Loper, E.. Natural language processing with Python. 1 ed.; O’Reilly; 2009. ISBN 9780596516499.
 27. Pedregosa, F., Michel, V., Grisel, O., Blondel, M., Prettenhofer, P., Weiss, R., Vanderplas, J., Courville, D., Pedregosa, F., Varoquaux, G., Gramfort, A., Thirion, B., Grisel, O., Dubourg, V., Passos, A., Brucher, M., Perrot andÉdouardand, M., Duchesnay, a., Duchesnay, F.. Scikit-learn: Machine Learning in Python. *Journal of Machine Learning Research* 2011;12:2825–2830. URL: http://scikit-learn.sourceforge.net.
 28. Appropriateness Criteria. URL: https://acsearch.acr.org/list?_ga=2.166544958.1866463646.1591622219-433059033.1577375860.

29. Geron, A.. Hands-on machine learning with Scikit-Learn and TensorFlow : concepts, tools, and techniques to build intelligent systems. ??? ISBN 1491962291.
30. Nair, V., Hinton, G.E.. Rectified Linear Units Improve Restricted Boltzmann Machines. In: *Proceedings of the 27th International Conference on Machine Learning*. Haifa, Isreal; 2010:432.
31. Hinton, G.E., Srivastava, N., Krizhevsky, A., Sutskever, I., Salakhutdinov, R.R.. Improving neural networks by preventing co-adaptation of feature detectors. Tech. Rep.; ???
32. Ioffe, S., Szegedy, C.. Batch normalization: Accelerating deep network training by reducing internal covariate shift. In: *32nd International Conference on Machine Learning, ICML 2015*; vol. 1. International Machine Learning Society (IMLS). ISBN 9781510810587; 2015:448–456.
33. Kingma, D.P., Ba, J.L.. Adam: A method for stochastic optimization. In: *3rd International Conference on Learning Representations, ICLR 2015 - Conference Track Proceedings*. International Conference on Learning Representations, ICLR; 2015:.
34. Murphy, K.P.. Machine Learning: A Probabilistic Perspective. 2012. ISBN 9780262018029. URL: http://link.springer.com/chapter/10.1007/978-94-011-3532-0_2. doi:10.1007/SpringerReference{_}35834.
35. American College of Radiology, . Acr manual on mri safety. ??? URL: <https://www.acr.org/-/media/ACR/Files/Radiology-Safety/MR-Safety/Manual-on-MR-Safety.pdf>.
36. Yu, J.P.J., Kansagra, A.P., Mongan, J.. The Radiologist's Workflow Environment: Evaluation of Disruptors and Potential Implications. *Journal of the American College of Radiology* 2014;11(6):589–593. URL: <http://www.sciencedirect.com/science/article/pii/S1546144013008508>. doi:10.1016/j.jacr.2013.12.026.
37. Balint, B.J., Steenburg, S.D., Lin, H., Shen, C., Steele, J.L., Gunderman, R.B.. Do Telephone Call Interruptions Have an Impact on Radiology Resident Diagnostic Accuracy? *Academic Radiology* 2014;21(12):1623–1628. URL: <http://www.sciencedirect.com/science/article/pii/S1076633214003079>. doi:10.1016/j.acra.2014.08.001.
38. Kansagra, A.P., Liu, K., Yu, J.P.J.. Disruption of Radiologist Workflow. *Current Problems in Diagnostic Radiology* 2016;45(2):101–106. URL: <http://www.sciencedirect.com/science/article/pii/S0363018815000869>. doi:10.1067/j.cpradiol.2015.05.006.
39. Fernandes, D.C.R., Poon, D., White, L.L., Andreyev, H.J.N.. What is the cost of delayed diagnosis of bile acid malabsorption and bile acid diarrhoea? *Frontline Gastroenterology* 2019;10(1):72–76. URL: <https://fg.bmj.com/content/10/1/72>. doi:10.1136/flgastro-2018-101011; publisher: British Medical Journal Publishing Group Section: Small bowel and Nutrition.
40. Ginocchio, L.A., Rogener, J., Chung, R., Xue, X., Tarnovsky, D., McMenemy, J.. Brainstorming Our Way to Improved Quality, Safety, and Resident Wellness in a Resource-Limited Emergency Department. *Current Problems in Diagnostic Radiology* 2020;URL: <http://www.sciencedirect.com/science/article/pii/S0363018820300530>. doi:10.1067/j.cpradiol.2020.03.005.

General Protocol Title	ACR Protocol Title	Local Protocol Title
head w/ w/o	mri head without and with iv contrast	mr brain wo + w cont
head w/ w/o	mri orbits without and with iv contrast	mr orbit(s) w/o + w cont
head w/ w/o	mri sella without and with iv contrast	mr sella w/o + w cont
head w/ w/o	mri head without and with iv contrast	mr brain stealth wo + w cont fh
head w/ w/o	mri head without and with iv contrast	mr sim brain with interp
head w/ w/o	mri head without and with iv contrast	mr brain gamma wo + w cont fh
head w/ w/o	mri head without and with iv contrast	mr brain intraop w cont w rad interp fh
head w/ w/o	mri head without and with iv contrast	ct preop head stealth mrk w cont
head w/ w/o	mri head perfusion with iv contrast	mr rcbv sequence
head w/ w/o	mri head and internal auditory canal without and with iv contrast	mr iac w/o + w cont
head w/ w/o	mr v head without and with iv contrast	mr mr v brain w/o & with cont
head w/ w/o	mra head without and with iv contrast	mr mra head w/o + w cont
head w/ w/o	mri orbit face neck without and with iv contrast	mr face w/o + w cont
head w/ w/o	mri orbit face neck without and with iv contrast	mr sim facial with interp
head w/ w/o	mri head without iv contrast with dti	mr brain w/o+w cont + dti
knee w/o	mri knee without iv contrast	mr knee lt w/o cont
knee w/o	mri knee without iv contrast	mr knee rt w/o cont
knee w/o	mri knee without iv contrast	mr pre-surg knee planning rt
knee w/o	mri knee without iv contrast	mr pre-surg knee planning lt
spine w/o	mri lumbar spine without iv contrast	mr l spine w/o cont
spine w/o	mri lumbar spine without iv contrast	mr l spine w/o cont chiro read cdi
spine w/o	mri thoracic and lumbar spine without iv contrast	mr t spine w/o cont
spine w/o	mri cervical spine without iv contrast	mr c spine w/o cont
spine w/o	mri cervical spine without iv contrast	mr c spine w/o cont chiro read cdi
spine w/ w/o	mri lumbar spine without iv contrast	mr l spine w/o + w cont
spine w/ w/o	mri thoracic and lumbar spine without and with iv contrast	mr t spine w/o + w cont
spine w/ w/o	mri thoracic and lumbar spine without and with iv contrast	mr sim thoracic spine with interp
spine w/ w/o	mri cervical spine without and with iv contrast	mr c spine w/o + w cont
spine w/ w/o	mri lumbar spine without and with iv contrast	mr sim lumbar spine with interp
shoulder w/o	mri shoulder without iv contrast	mr shoulder lt w/o cont
shoulder w/o	mri shoulder without iv contrast	mr shoulder rt w/o cont
shoulder w/o	mri shoulder without iv contrast	mr scapula lt w/o cont
shoulder w/o	mri shoulder without iv contrast	mr scapula rt w/o cont

shoulder w/o	mri brachial plexus without iv contrast	mr brach plex rt w/o cont
shoulder w/o	mri brachial plexus without iv contrast	mr brach plex lt w/o cont
hand w/o	mri hand without iv contrast	mr hand lt w/o cont
hand w/o	mri hand without iv contrast	mr finger lt w/o cont
hand w/o	mri hand without iv contrast	mr finger rt w/o cont
hand w/o	mri hand without iv contrast	mr hand rt w/o cont
cardiac w/ w/o	mri heart function and morphology without and with iv contrast	mr cardiac morph-func w/o + w cont
cardiac w/ w/o	mri heart with stress without and with iv contrast	mr cardiac morph func w/stress w/o + w cont fh
head w/o	mri head without iv contrast	mr brain w/o cont
head w/o	mri head without iv contrast	mr memory loss brain w/o cont w 3d imaging
head w/o	mri head without iv contrast	mr neuroreader brain w/o cont w 3d imaging
head w/o	mri head without iv contrast	mr tmj bilat
head w/o	mri head without iv contrast	mr brain stealth wo cont fh
head w/o	mri head without iv contrast	ct preop head stealth mrk w/o cont
head w/o	mri head without iv contrast	mr brain w/o cont ltd research fh
head w/o	mri head without iv contrast	mr brain intraop w/o cont with rad interp fh
head w/o	mri head without iv contrast	mr tmj lt
head w/o	mri head without iv contrast	mr meg brain w/o cont
head w/o	mri head without iv contrast	mr tmj rt
head w/o	mri head without iv contrast	ct head stealth mrk w/o cont
head w/o	mri head without iv contrast	mr brain gamma wo cont fh
head w/o	mra head without iv contrast	mr mra head w/o cont
head w/o	mri orbits without iv contrast	mr orbit(s) w/o cont
head w/o	mri functional (fmri) head without iv contrast	mr functional tech testing fh
head w/o	mr spectroscopy head without iv contrast	mr spectroscopy
head w/o	mrsv head without iv contrast	mr mrsv brain w/o cont.
head w/o	mri orbit face neck without iv contrast	mr face w/o cont
foot w/ w/o	mri foot without and with iv contrast	mr foot lt w/o + w cont
foot w/ w/o	mri foot without and with iv contrast	mr foot rt w/o + w cont
foot w/ w/o	mri foot without and with iv contrast	mr toes lt w/o + w cont
foot w/ w/o	mri foot without and with iv contrast	mr forefoot rt w/o + w cont
foot w/ w/o	mri foot without and with iv contrast	mr forefoot lt w/o + w cont
foot w/ w/o	mri foot without and with iv contrast	mr toes rt w/o + w cont
foot w/ w/o	mri ankle and hindfoot without and with iv contrast	mr heel rt w/o + w cont
foot w/o	mri foot without iv contrast	mr foot rt w/o cont
foot w/o	mri foot without iv contrast	mr foot lt w/o cont
foot w/o	mri foot without iv contrast	mr forefoot lt w/o cont
foot w/o	mri foot without iv contrast	mr forefoot rt w/o cont
foot w/o	mri foot without iv contrast	mr toes rt w/o cont
foot w/o	mri foot without iv contrast	mr toes lt w/o cont
foot w/o	mri ankle and hindfoot without iv contrast	mr hindfoot lt w/o cont
foot w/o	mri ankle and hindfoot without iv contrast	mr hindfoot rt w/o cont

foot w/o	mri ankle and hindfoot without iv contrast	mr heel rt w/o cont
foot w/o	mri ankle and hindfoot without iv contrast	mr heel lt w/o cont
shoulder w/	mr arthrography shoulder	mr shoulder lt w cont
shoulder w/	mr arthrography shoulder	mr shoulder rt w cont
pelvis w/ w/o	mri sacroiliac joints without and with iv contrast	mr sacrum w/o + w contrast
pelvis w/ w/o	mri pelvis without and with iv contrast	mr prostate w/o + w cont
pelvis w/ w/o	mri pelvis without and with iv contrast	mr pelvis msk w/o + w cont
pelvis w/ w/o	mri pelvis without and with iv contrast	mr pelvis organ w/o + w cont
pelvis w/ w/o	mri pelvis without and with iv contrast	mr sim pelvis with interp
pelvis w/ w/o	mr enterography	mr enterography w/o + w cont
pelvis w/ w/o	mri hip without and with iv contrast	mr hip rt w/o + w cont
pelvis w/ w/o	mri hip without and with iv contrast	mr hip lt w/o + w cont
pelvis w/ w/o	mra abdomen and pelvis with iv contrast	mr mra pelvis
pelvis w/o	mri hip without iv contrast	mr hip lt w/o cont
pelvis w/o	mri hip without iv contrast	mr hip rt w/o cont
pelvis w/o	mri sacroiliac joints without iv contrast	mr sacrum w/o
pelvis w/o	mri sacroiliac joints without iv contrast	mr sacrum w/o chiro read cdi
pelvis w/o	mri pelvis without iv contrast	mr pelvis msk w/o cont
pelvis w/o	mri pelvis without and with iv contrast	mr pelvis ltd fibroid protocol cdi
pelvis w/o	mri pelvis without iv contrast	mr pelvis organ w/o cont
abdomen w/ w/o	mri abdomen without and with iv contrast	mr abd w/o + w cont
abdomen w/ w/o	mri abdomen without and with iv contrast	mr sim abd with interp
abdomen w/ w/o	mri abdomen and pelvis without and with iv contrast	mr abd/pelvis w + w/o cont
abdomen w/ w/o	mra abdomen without and with iv contrast	mr mra abdomen w/o + w cont
abdomen w/ w/o	mr elastography abdomen	mr abd w + w/o + elastography
thigh w/o	mri lower extremity area of interest (not pelvis or hip) without iv contrast	mr femur lt w/o cont
thigh w/o	mri lower extremity area of interest (not pelvis or hip) without iv contrast	mr femur rt w/o cont
extremity w/o	mri lower extremity area of interest (not pelvis or hip) without iv contrast	mr tib/fib rt w/o cont
extremity w/o	mri lower extremity area of interest (not pelvis or hip) without iv contrast	mr low ext lt multi w/o cont
extremity w/o	mra lower extremity without iv contrast	mr tib/fib lt w/o cont
extremity w/o	mri extremity area of interest without iv contrast	mr humerus rt w/o cont
extremity w/o	mri extremity area of interest without iv contrast	mr humerus lt w/o cont

extremity w/o	mri extremity area of interest without iv contrast	mr forearm lt w/o cont
extremity w/o	mri extremity area of interest without iv contrast	mr forearm rt w/o cont
extremity w/o	mra extremity area of interest without and with iv contrast	mr sim ext upper with interp
neck w/	mra neck with iv contrast	mr mra neck w cont
breast w/ w/o	mri breast without and with iv contrast bilateral	bi mr breast bilat w/o+w cont with cad
breast w/ w/o	image-guided core biopsy breast	bi mr guide breast bx w w/o clip+spec 1st lesion rt
breast w/ w/o	image-guided core biopsy breast	bi mr guide breast bx w w/o clip+spec 1st lesion lt
breast w/ w/o	image-guided core biopsy breast	bi mr guide breast bx w w/o clip+spec 1st lesion bi
breast w/ w/o	mri breast without and with iv contrast	bi mr breast lt w/o+w cont with cad
breast w/ w/o	mri breast without and with iv contrast	bi mr breast rt w/o+w cont with cad
ankle w/o	mri ankle without iv contrast	mr ankle lt w/o cont
ankle w/o	mri ankle without iv contrast	mr ankle rt w/o cont
ankle w/o	mri ankle and hindfoot without iv contrast	mr ankle achilles lt w/o cont
ankle w/o	mri ankle and hindfoot without iv contrast	mr ankle achilles rt w/o cont
wrist w/o	mri wrist without iv contrast	mr wrist rt w/o cont
wrist w/o	mri wrist without iv contrast	mr wrist lt w/o cont
pelvis w/	mr arthrography hip	mr hip rt w cont
pelvis w/	mr arthrography hip	mr hip lt w cont
pelvis w/	mri pelvis without and with iv contrast	mr pelvis organ w/cont
pelvis w/	mra extremity area of interest without and with iv contrast	mr mra pelvis + low ext bilat run off w cont
cardiac w/o	mri heart function and morphology without iv contrast	mr cardiac morph + func w/o
shoulder w/ w/o	mri brachial plexus without and with iv contrast	mr brach plex lt w/o + w cont
shoulder w/ w/o	mri brachial plexus without and with iv contrast	mr brach plex rt w/o + w cont
shoulder w/ w/o	mri shoulder without and with iv contrast	mr scapula lt w/o + w cont
shoulder w/ w/o	mri shoulder without and with iv contrast	mr shoulder rt w/o + w cont
shoulder w/ w/o	mri shoulder without and with iv contrast	mr shoulder lt w/o + w cont
shoulder w/ w/o	mri shoulder without and with iv contrast	mr scapula rt w/o & with cont
extremity w/ w/o	mri extremity area of interest without and with iv contrast	mr humerus rt w/o + w cont
extremity w/ w/o	mri extremity area of interest without and with iv contrast	mr humerus lt w/o + w cont
extremity w/ w/o	mri extremity area of interest without and with iv contrast	mr forearm rt w/o & with cont
extremity w/ w/o	mri extremity area of interest without and with iv contrast	mr forearm lt w/o + w cont

extremity w/ w/o	mri extremity area of interest without and with iv contrast	mr mra upp ext rt multi w/o + w cont
extremity w/ w/o	mri lower extremity area of interest (not pelvis or hip) without and with iv contrast	mr tib/fib lt w/o + w cont
extremity w/ w/o	mri lower extremity area of interest (not pelvis or hip) without and with iv contrast	mr tib/fib rt w/o + w cont
extremity w/ w/o	mri lower extremity area of interest (not pelvis or hip) without and with iv contrast	mr low ext lt multi w/o + w cont
extremity w/ w/o	mri lower extremity area of interest (not pelvis or hip) without and with iv contrast	mr sim ext lower with interp
extremity w/ w/o	mra lower extremity without and with iv contrast	mr mra low ext lt multi w/o + w cont
neck w/ w/o	mri neck without and with iv contrast	mr neck soft tissue w/o + w cont
neck w/ w/o	mri neck without and with iv contrast	mr sim neck with interp
spine w/	mri lumbar spine without and with iv contrast	mr l spine w cont
spine w/	mri cervical spine with iv contrast	mr c spine w cont
spine w/	mri thoracic and lumbar spine without and with iv contrast	mr t spine w cont
elbow w/o	mri elbow without iv contrast	mr elbow rt w/o cont
elbow w/o	mri elbow without iv contrast	mr elbow lt w/o cont
whole body w/o	mri whole body without iv contrast	mr whole body survey
thigh w/ w/o	mri lower extremity area of interest (not pelvis or hip) without and with iv contrast	mr femur rt w/o + w cont
thigh w/ w/o	mri lower extremity area of interest (not pelvis or hip) without and with iv contrast	mr femur lt w/o + w cont
chest w/o	mri chest without iv contrast	mr chest w/o cont
chest w/o	mra chest without iv contrast	mr mra chest w/o cont
mrcp	mri abdomen without and with iv contrast with mrcp	mr mrcp w/o + w cont
mrcp	mri abdomen without iv contrast with mrcp	mr mrcp w/o cont
abdomen w/o	mri abdomen without iv contrast	mr abd w/o cont
abdomen w/o	mri abdomen without iv contrast	mr abd w/o cont ltd for iron content fh
abdomen w/o	mri abdomen without iv contrast	mr abd w/o cont ltd research fh
head w/	mrsv head with iv contrast	mr mrsv brain with cont
head w/	mri orbit face neck without and with iv contrast	mr orbit(s) w cont
head w/	mri head with iv contrast	mr brain w cont
head w/	mri head without and with iv contrast	ct head stealth mrk w cont
head w/	mri head without and with iv contrast	mr brain gamma w cont fh
neck w/o	mra neck without iv contrast	mr mra neck w/o cont
neck w/o	mri neck without iv contrast	mr neck w/o cont

ankle w/ w/o	mri ankle without and with iv contrast	mr ankle rt w/o + with cont
ankle w/ w/o	mri ankle without and with iv contrast	mr ankle lt w/o + with cont
wrist w/	mr arthrography wrist	mr wrist rt w cont
wrist w/	mr arthrography wrist	mr wrist lt w cont
chest w/ w/o	mri chest without and with iv contrast	mr chest w/o + w cont
chest w/ w/o	mri chest without and with iv contrast	mr sim chest with interp
chest w/ w/o	mra chest without and with iv contrast	mr mra chest w/o + w cont
hand w/ w/o	mri hand without and with iv contrast	mr hand rt w/o + w cont
hand w/ w/o	mri hand without and with iv contrast	mr hand lt w/o + w cont
hand w/ w/o	mri hand without and with iv contrast	mr finger lt w/o + w cont
hand w/ w/o	mri hand without and with iv contrast	mr finger rt w/o + w cont
knee w/ w/o	mri knee without and with iv contrast	mr knee lt w/o + w cont
knee w/ w/o	mri knee without and with iv contrast	mr knee rt w/o + w cont
knee w/ w/o	mra knee without and with iv contrast	mr mra bilat knee popliteal entrapment wo + w cont
wrist w/ w/o	mri wrist without and with iv contrast	mr wrist lt w/o + w cont
wrist w/ w/o	mri wrist without and with iv contrast	mr wrist rt w/o + w cont
breast w/o	mri breast without iv contrast bilateral	bi mr breast bilat w/o cont
breast w/o	image-guided transthoracic needle biopsy	mr guide needle placement
breast w/o	mri breast without iv contrast	bi mr breast rt w/o cont
elbow w/	mr arthrography elbow	mr elbow lt w cont
elbow w/	mr arthrography elbow	mr elbow rt w cont
elbow w/ w/o	mri elbow without and with iv contrast	mr elbow rt w/o + w cont
elbow w/ w/o	mri elbow without and with iv contrast	mr elbow lt w/o + w cont
abdomen w/	mra abdomen without and with iv contrast	mr mra abdomen w cont
knee w/	mr arthrography knee	mr knee rt w cont
knee w/	mr arthrography knee	mr knee lt w cont
chest w/	mra chest without and with iv contrast	mr mra chest w cont
ankle w/	mr arthrography ankle	mr ankle lt w cont
hand w/	mr arthrography wrist	mr hand rt w cont
hand w/	mr arthrography wrist	mr hand lt w cont

Table 3: Local protocol titles with corresponding ACR and general protocol titles.